ISSN 0965-5441, Petroleum Chemistry, 2024, Vol. 64, No. 5, pp. 540–547. © Pleiades Publishing, Ltd., 2024.
ISSN 0965-5441, Petroleum Chemistry, 2024. © Pleiades Publishing, Ltd., 2024.

Effect of Ultrasonic Treatment on the Properties and Composition of High-Wax Crude Oil and Its Precipitates

G. I. Volkova[a],*, D. A. Zubarev[a], and P. B. Kadychagov[a]

[a] *Institute of Petroleum Chemistry, Siberian Branch, Russian Academy of Sciences, Tomsk, 634055 Russia*
**e-mail: galivvol@yandex.ru*

Received September 21, 2023; revised January 24, 2024; accepted February 27, 2024

Abstract—High-wax crude oil was treated with ultrasound (sample weight 50 g, frequency 22 kHz, field intensity 8 W/cm^2) for 10 min. The ultrasonic treatment led to an increase in the crude oil viscosity, viscous flow activation energy, specific energy of the break of the disperse system, congealing point, pour point, and precipitate amount and to changes in the precipitate structure. The oil fraction of the crude oil, precipitates, and raffinates was analyzed by IR spectroscopy and chromatography–mass spectrometry. The content of high-molecular-mass *n*-alkanes in oils from the precipitate of the ultrasonically treated crude oil considerably decreases.

Keywords: high-wax crude oil, ultrasonic treatment, viscosity, precipitate, raffinate, *n*-alkanes

DOI: 10.1134/S0965544124020026

Petroleum still remains the most important source of energy, ensuring the growth of the world economy [1]. According to the data of the International Energy Agency, petroleum still plays the leading role in the energy production in the world; its share is 30% [2]. In the total balance of hydrocarbons, waxy and high-wax crude oils make up more than 20% [3]. The major fraction of waxy crude oils in Russia are extracted from fields with low ambient temperature. More than 30% of the proven reserves of crude oil in Russia are located in the permafrost region, which is actually the fuel and energy base [4].

The microstructure of crude oils with high content of high-molecular-mass paraffins significantly changes with a decrease in the temperature owing to the growth and subsequent sedimentation of crystals. Involvement of deposits of hard-to-recover crude oils, including high-wax crude oils [5], into the development becomes more and more pressing problem. According to Rosnedra's estimates, by 2030 the petroleum extraction from nontraditional sources can reach 10–20% of the total hydrocarbon recovery volume [6].

The most efficient procedures for extracting hard-to-recover crude oils are upgraded technologies used for the extraction of traditional crude oils, including thermal [7], chemical [1, 8–11], and physical [12–17] methods, rather than newly developed technologies. Particular attention is paid to the physical and physicochemical methods of action on petroleum systems to improve their structural and mechanical properties. Environmentally clean wave treatment methods, in particular, ultrasonic treatment (UST), show promise [17]. Ultrasonic treatment proved to be efficient for reducing the viscosity and congealing point of low-wax and waxy resinous crude oils [18, 19] and for increasing the petroleum recovery factor, especially from depleted strata [20–22]. As noted in [22], the UST advantages are the possibility of wide use, high efficiency, environmental cleanness, and low cost. Dengaev et al. [23] analyzed papers dealing with chemical transformations of petroleum components under the action of ultrasound and concluded that further studies are required to understand how ultrasonic technologies affect the petroleum properties.

Significant differences in the group composition of crude oil oils to not allow a priori estimation of the effect exerted by one or another kind of treatment on the composition and structural-mechanical properties both of crude oils and of precipitates inevitably formed in the course of extraction and transportation of hydrocarbon feedstock. This study deals with the effect of ultrasonic treatment on the structural-mechanical properties of high-wax low-resin crude oil and on the composition of the dispersed phase (precipitate) and dispersion medium (raffinate) after the precipitation.

EXPERIMENTAL

Chemicals. The following chemicals were used in the study: *n*-hexane (Ekos-1, Russia), benzene (Ekos-1), ethanol (Vekton, Russia), silica gel ASA (0.25–0.50 mm) (Hong Kong Chemical Corporation, Hong Kong), trichloromethane (Ekos-1, Russia), and deuteroacenaphthene (Sigma–Aldrich, Switzerland).

Investigation objects. As an investigation object, we used high-wax low-resin crude oil with the congealing point of +20°C, containing 97.8 wt % oils (including 9.8 wt % *n*-alkanes), 2.2 wt % silica gel resins, and traces of asphaltenes. The component composition of the initial and ultrasonically treated crude oils was determined by standard procedures [24].

The crude oil was ultrasonically treated using a UZDN-T ultrasonic disintegrator. The installation contains a magnetostriction converter operating at 22 kHz and a rod waveguide with the working end diameter of 1.71 cm and end area of 2.295 cm^2. The acoustic power of vibrations absorbed by water was estimated by the calorimetric method [25]. The ultrasound intensity at the converter end radius of 0.86 cm was 8 W/cm^2. A 0.05-g portion of the crude oil was treated for 10 min at the ambient temperature of 20°C.

From the initial and ultrasonically treated samples, we isolated the dispersed phase (precipitate) and dispersion medium (raffinate). The precipitation was performed using an installation operating on the "cold rod" principle. Experiment conditions: rod temperature 14°C, temperature of the external medium 35°C, experiment time 1 h, sample weight 40 g. The amount of the precipitate formed on the rod was estimated gravimetrically.

Investigation methods. The rheological parameters of the samples were determined with a HAAKE Viscotester iQ rotary viscometer. The viscosity–temperature dependences were obtained in the course of continuous cooling at a rate of 1 deg/min at a constant shear rate of 1 s^{-1}, at which the breakdown of the thixotropic system structure was minimal. The viscous flow activation energy (E_a) was determined from the slopes of the linear portions in the plots of the logarithm of effective viscosity (μ) vs. reciprocal temperature ($\ln \mu = f(1/T)$) [26].

The isothermal flow curves were recorded in the ascending and descending modes at a temperature of 22°C at which *n*-alkanes start to actively crystallize. The specific energy of the breakdown of the supramolecular structure of the disperse system (ΔW) was calculated from the area of the hysteresis loop formed by the ascending and descending flow curves [27].

The IR spectra of the crude oil, precipitates, raffinates, and their oil fractions were recorded with a Nicolet 5700 FTIR spectrometer. Samples were applied as a film onto KBr plates from a solution in trichloromethane. OMNIC 7.2 Thermo Nicolet Corporation software was used for processing the IR spectra and determining the optical density. We determined the optical density (D) for the characteristic absorption bands of the following bonds: $C{=}C_{arom}$ (1600 cm^{-1}), $(-CH_3)_{\delta as}$ (1465 cm^{-1}), $(-CH_3)_{\delta s}$ (1380 cm^{-1}), $-CH_2-$ (720 cm^{-1}). We calculated the following spectral coefficients: C_1, aromaticity (D_{1600}/D_{1465}); C_2, branching (D_{1380}/D_{1465}); C_3, content of polymethylene sequences with more than four carbon atoms (D_{720}/D_{1465}); C_4, aliphaticity ($(D_{720}+D_{1380})/D_{1600}$); and C_5, content of naphthene structures (D_{975}/D_{720}).

The oil fraction of the crude oil, precipitates, and raffinates was analyzed by gas chromatography–mass spectrometry (GC-MS) with a DFS magnetic device (Thermo Scientific, Germany). The chromatograph operation conditions were as follows: Agilent quartz capillary chromatographic column 0.25 mm i.d., 30 m long, stationary phase DB-35MS; carrier gas helium, flow rate 1.0 mL/min; thermostat temperature 250°C; interface temperature 270°C; thermostat heating schedule: t_{init} = 80°C, isotherm for 2 min, heating at a rate of 3 deg/min to t_{max} = 300°C, and keeping at the final temperature for 25 min. Mass spectrometer operation conditions: electron impact, ionizing electron energy 70 eV, ionization chamber temperature 250°C, mass range recorded 50–500 amu, and spectrum sweeping time 1 s.

The chromatograms of the organic components were constructed in the total ion current (TIC) and selected-ion monitoring (SIM) modes using the XCalibur program. The compounds were identified by computer search in libraries using the NIST-05 mass-spectral library (National Institute of Standards and Technology, the United States; more than 200 thousand compounds). Quantitative calculations were based on the chromatographic peak areas, with deuteroacenaphthene used as an internal reference. The mass fragmentograms for *n*-alkanes, naphthenes, and *n*-alkylbenzenes were constructed using the characteristic ions with m/z = 57, 82, and 92, respectively.

The congealing point (T_c) of the samples was determined with a Crystal device (Institute of Petroleum

Table 1. Viscosities and congealing and crystallization points of crude oil samples

Sample	Viscosity, mPa s					Temperature[b], °C			
	shear rate, s^{-1} [a]		temperature,°C			T_c	T_1	T_2	T_3
	4	80	21	17	15				
C	253	60	100	2300	9200	16.8	20.1	19.4	14.8
C_u	1365	118	40	3320	No flow	17.6	20.5	19.6	15.8

[a] At 22°C.

[b] Temperatures: T_1, onset of formation of primary paraffin crystals; T_2, spontaneous growth of primary crystals; T_3, formation of a continuous crystalline network.

Chemistry, Siberian Branch, Russian Academy of Sciences).

The microstructure of the samples was examined by transmission optical microscopy (AXIO LAB.A1).

The following sample designations were used: *C*, crude oil; C_u, ultrasonically treated crude oil; *P*, crude oil precipitate; P_u, precipitate of ultrasonically treated crude oil; O_c, oil fraction of the crude oil; O_c_u, oil fraction of the ultrasonically treated crude oil; O_p, oil fraction of the crude oil precipitate; O_p_u, oil fraction of the precipitate of ultrasonically treated crude oil; O_r, oil fraction of the raffinate; and O_r_u, oil fraction of the raffinate of ultrasonically treated crude oil.

RESULTS AND DISCUSSION

Viscosity–Temperature Characteristics of the Crude Oil

Ultrasonic treatment of high-wax crude oil leads to changes in its structural and mechanical properties. After UST, the congealing point of C_u increases from 16.8 to 17.6°C.

The dynamic viscosity of the crude oil (sample *C*) at 22°C decreases from 253 (shear rate 4 s^{-1}) to 60 mPa s (shear rate 80 s^{-1}). Sample C_u is more structured: At low shear rates, at which the three-dimensional structure of paraffin crystals is not broken, the viscosity of C_u is 5.4 times higher than that of *C* (Table 1). At high shear rates (80 s^{-1}), the difference in the viscosity is less pronounced, but the viscosity of C_u is still 2 times higher than that of *C*.

The viscosity–temperature characteristics of the crude oil before and after UST are presented in Table 1 and Fig. 1. The temperature dependences of the viscosity for samples *C* and C_u, recorded at a shear rate of 1 s^{-1}, consist of three portions. The viscosity of the crude oils does not noticeably increase in the temperature interval 22–30°C, and sample C_u in this interval is less viscous than *C*. As the temperature is decreased further, the viscosity of both samples gradually increases owing to the formation of paraffin crystals (T_1). The viscosity of C_u increases more intensely. This is followed by a sharp increase in the viscosity due to the growth of primary crystals (T_2), followed by the formation of a continuous crystalline network (T_3). The viscosity in the narrow temperature interval increases by 330 and 390 mPa s for samples *C* and C_u, respectively. Below 20°C, the viscosity of the ultrasonically treated crude oil is, on the average, 1.4 times higher than that of the initial crude oil down to the pour point. Processing of the viscosity–temperature curves in the coordinates $\ln \mu = f(1/T)$ showed that the crystallization onset points were 20.1 and 20.5, and the pour points, 14.8 and 15.8°C for samples *C* and C_u, respectively (Table 1).

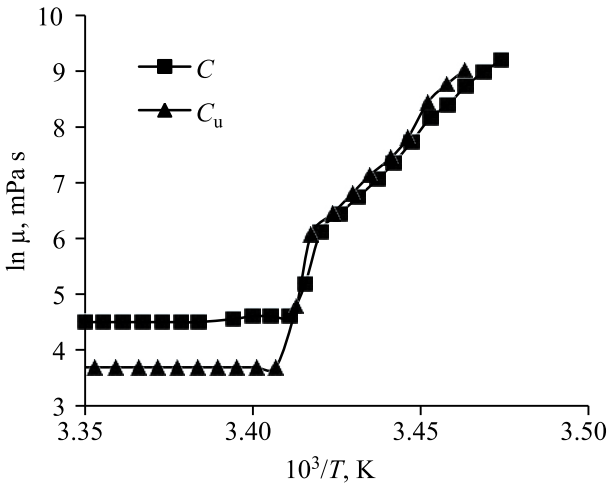

Fig. 1. Semilog plot of the effective viscosity (μ) of the crude oil before and after ultrasonic treatment vs. reciprocal temperature at a shear rate of 1 s^{-1}.

Table 2. Viscous flow activation energy of the crude oils

Sample	Viscous flow activation energy, kJ/mol		
	E_{a1}[a]	E_{a2}[b]	E_{a3}[c]
C	6	1668	494
C_u	0	1859	505

[a] E_a at 293–298 K.
[b] E_a at 292–293 K.
[c] E_a at 288–293 K.

The viscous flow activation energy for the initial and ultrasonically treated high-wax crude oil (E_{a1}) at temperatures exceeding 20°C is close to zero (Table 2). The crystal nucleation and growth occur more actively in the ultrasonically treated crude oil (E_{a2}). As the temperature is decreased further, the structure formation and break processes occur at equal rates, which leads to approximately equal activation energies of viscous flow in the temperature interval 288–293 K (E_{a3}) at considerably higher viscosity of C_u (Table 1).

The strength of the structures formed in samples C and C_u (22°C) can be characterized by the specific energy of the break of the disperse system. This quantity can be determined by calculating the area of the hysteresis loop formed by the ascending and descending isothermal flow curves (Fig. 2). The hysteresis phenomena in thixotropic systems are usually attributed to insufficient break of the initial structure or to delayed restoration of the broken structure. Deviation from the equilibrium flow state is believed to be the main cause of the hysteresis [28]. UST enhances the strength of the initial crude oil structure, as follows from the ΔW values: 13 and 23 kJ/m^3 for C and C_u, respectively.

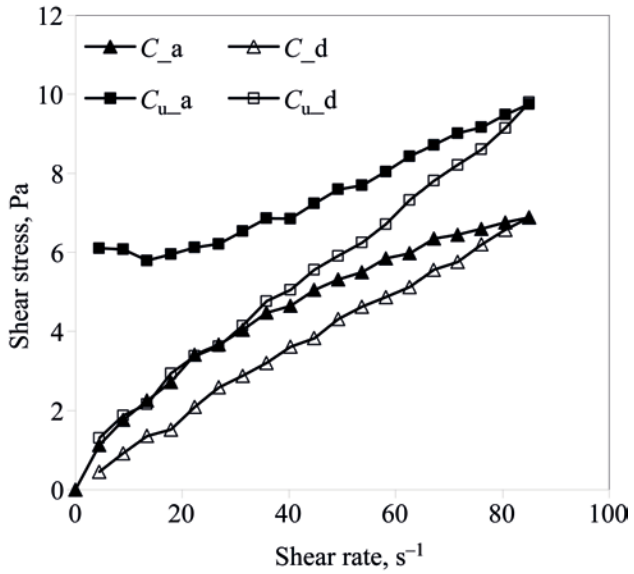

Fig. 2. Ascending (a) and descending (d) isothermal flow curves of the crude oil at 22°C.

Structure of precipitates. The UST affects the precipitate formation in the high-wax crude oil. The weight of the precipitate separated from the crude oil after UST increases from 6.8 to 12.6 g/100 g for C and C_u, respectively. The precipitate from the initial crude oil, P, consists of needle-like formations up to 50 μm long, forming star-shaped structures; after UST, shorter needle-like crystals (up to 20 μm, sample P_u) are formed (Fig. 3).

Structural-group composition of the samples. According to the IR data, the content of aromatic structures (C_1), branching (C_2), content of polymethylene sequences with more than four carbon atoms (C_3), and content of naphthene structures (C_5) in the ultrasonically treated crude oil (sample C_u) decreases, whereas the aliphaticity (C_4) increases relative to sample C (Table 3).

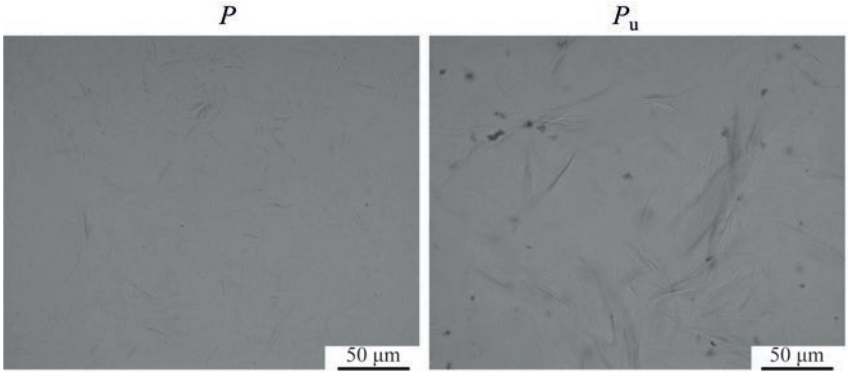

Fig. 3. Photomicrographs of the precipitates.

Table 3. Spectral parameters of the samples

Sample	Spectral parameters, rel. units				
	C_1	C_2	C_3	C_4	C_5
C	0.22	0.53	0.29	13.35	0.19
C_u	0.21	0.47	0.24	13.84	0.18
P	0.20	0.49	0.28	13.70	0.17
P_u	0.19	0.43	0.24	14.84	0.16
R	0.20	0.48	0.25	14.18	0.18
R_u	0.21	0.50	0.27	13.92	0.19

Table 4. Spectral parameters of the oil fraction of the samples

Sample	Spectral parameters, rel. units	
	C_2	C_3
O_c	0.48	0.31
O_c_u	0.52	0.37
O_p	0.28	0.41
O_p_c	0.38	0.42
O_r	0.53	0.29
O_r_c	0.46	0.26

For the precipitates (samples P and P_u), the trend is similar, but the aliphaticity (C_4) of sample P_u increases to a greater extent. In the raffinate (sample R_u compared to R), on the contrary, the content of structural fragments described by the parameters C_1, C_2, C_3, and C_5 increases, whereas the aliphaticity (C_4) decreases.

Composition and structure of the oil fraction. We isolated the oil fractions from the crude oil, precipitates, and raffinates and analyzed them by IR spectroscopy and GC-MS.

The oils isolated from the ultrasonically treated crude oil (O_c_u) have higher content of branched structures

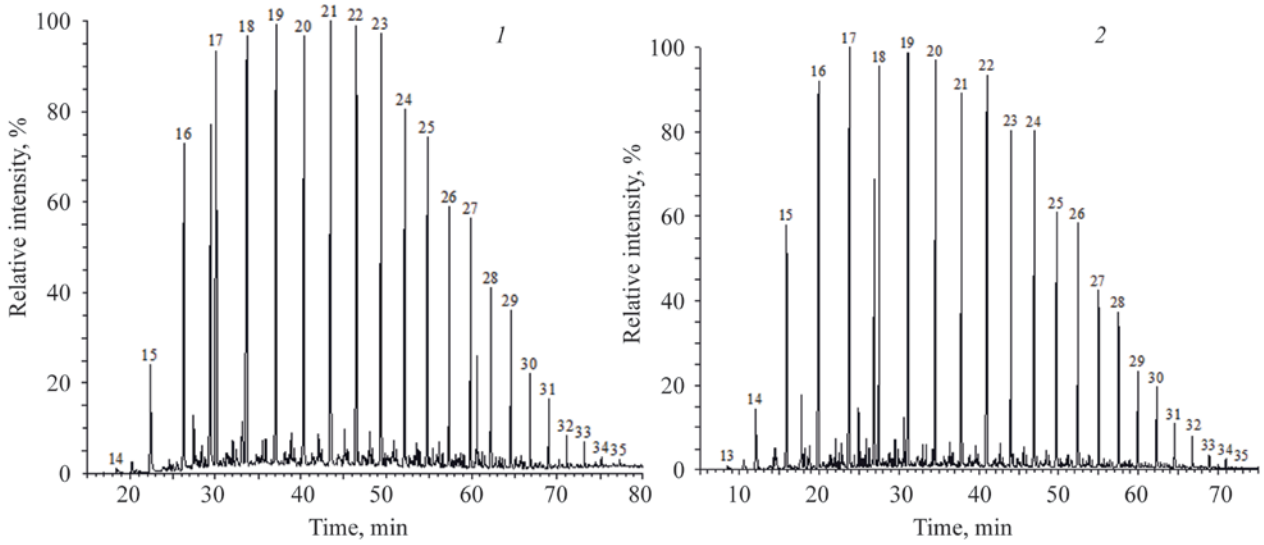

Fig. 4. SIM (m/z = 57) chromatograms of the oil fraction, samples (*1*) O_c and (*2*) O_c_u. Numerals at peaks correspond to the total number of carbon atoms in the molecule.

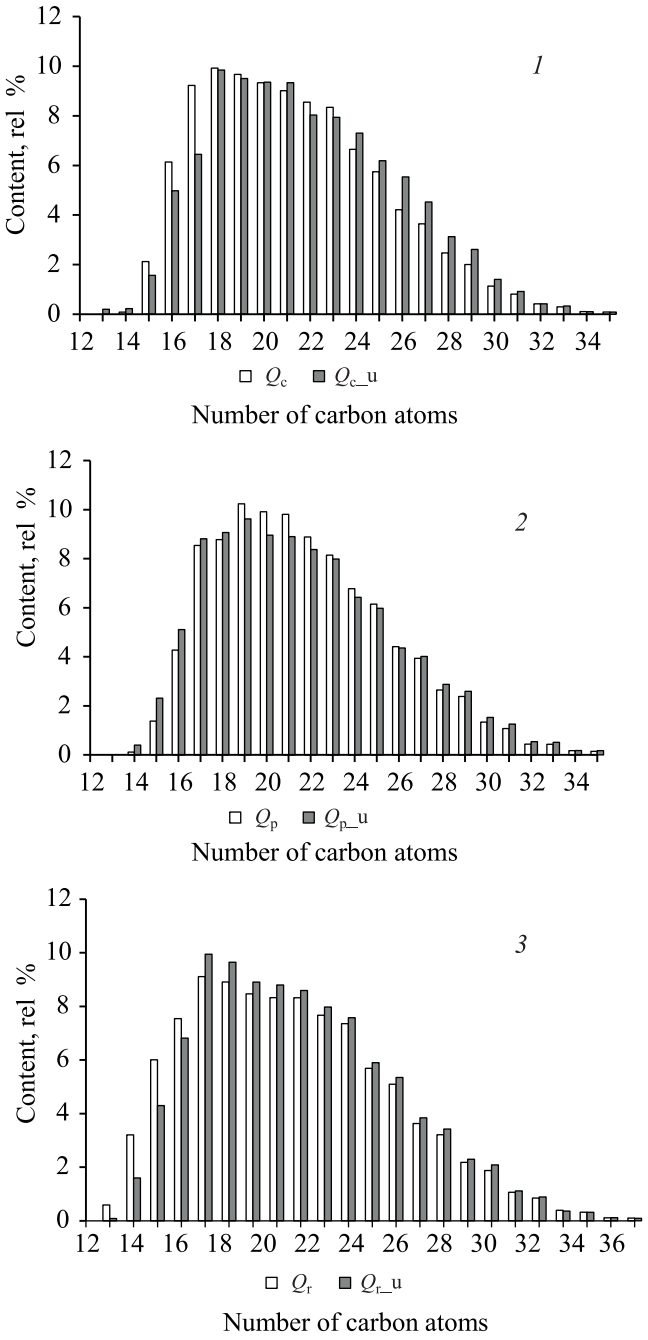

Fig. 5. Molecular-mass distribution of *n*-alkanes: (*1*) crude oil, (*2*) precipitate, and (*3*) raffinate.

(C_2) and polymethylene sequences (C_3) compared to O_c (Table 4). In the oils isolated from the precipitates of ultrasonically treated crude oil (O_p_u), the parameters C_2 and C_3 are also higher. The oils from the raffinates, compared to those from the precipitates, have higher content of branched structures (C_2) and lower content of polymethylene sequences. Sample O_r_u isolated from the raffinate of the ultrasonically treated crude oil has lower content of branched and long-chain fragments compared to O_r.

The content of *n*-alkanes in the oil fractions of the samples was determined by GC-MS. Figures 4 and 5 show the SIM (*m/z* = 57) chromatograms of oil fractions O_c (*1*) and O_c_u (*2*) and the molecular-mass distribution (MMD) of *n*-alkanes in the crude oil, precipitates, and raffinates. The MMD of *n*-alkanes from both the initial and ultrasonically treated samples is unimodal with the maxima corresponding to $C_{18}H_{38}$, $C_{19}H_{40}$, and $C_{17}H_{36}$ for the crude oil, precipitate, and raffinate, respectively. After the ultrasonic treatment, the C_{13} homolog is detected in the oil fraction of the crude oil (O_c_u).

The *n*-alkanes detected were subdivided into three groups: low-melting (C_{10}–C_{15}), medium-melting (C_{16}–C_{22}), and high-melting (high-molecular-mass) (Table 5). The major components of the oil fraction of all the samples are *n*-alkanes of the $\sum C_{16}$–C_{22} group. The lowest content of this group is observed in sample O_c_u, and the highest content, in O_c. The content of low-melting *n*-alkanes in the oils varies in a wide range: The highest content is observed in the raffinates, and the lowest content, in the precipitate (sample O_p). The relative content of high-molecular-mass *n*-alkanes in the oil fractions of the raffinates (O_r, O_r_u) is minimal. After UST of the crude oil, the content of the $\sum > C_{22}$ groups in oils of the crude oil (O_c_u) and raffinates (O_r_u) increases, whereas in oils of the precipitates (O_p-c) it does not change. The ratio of the sum of high-molecular-mass *n*-alkanes to low-molecular-mass alkanes in oils of the raffinates (O_r, O_r_u) is the lowest. In oils of the precipitates after UST (O_p_u), the relative content of high-molecular-mass *n*-alkanes is considerably lower, which will positively influence the congealing point of paraffin deposits, despite larger amount of the precipitate after UST.

We have determined the content of naphthenes (N) and *n*-alkylbenzenes (AB) in oil samples O_c and O_c_u. The relative content of the identified naphthenes in the oil fraction of the crude oil after the ultrasonic treatment decreases almost by half (284 and 152 μg). The relative content of the low-molecular-mass group of naphthenes increases from 7 to 23 wt %, but the amount of high-molecular-mass naphthenes appreciably decreases (Table 6).

The total content of *n*-alkylbenzenes in the initial crude oil is considerably lower (53 μg) than that of naphthenes and decreases to 8 μg in the ultrasonically

Table 5. Content of *n*-alkanes in the oil fraction of the samples

Sample	Relative content of *n*-alkane subgroups, wt %			$\sum>C_{22}/\sum C_{10}–C_{15}$
	$\sum C_{10}–C_{15}$	$\sum C_{16}–C_{22}$	$\sum>C_{22}$	
O_c	2.2	61.9	35.9	16.3
O_c_u	2	57.5	40.5	20.3
O_p	1.5	60.5	38.1	25.5
O_p_u	2.7	58.9	38.4	14.2
O_{pr}	9.8	58.3	31.9	3.3
O_r-U	6.0	60.7	33.4	5.6

Table 6. Content of naphthenes and *n*-alkylbenzenes in the oil fraction of the samples

Sample	Content of subgroups, wt %						$\sum>C_{22}/\sum C_{10}–C_{15}$	
	$\sum C_{10}–C_{15}$		$\sum C_{16}–C_{22}$		$\sum>C_{22}$			
	N	AB	N	AB	N	AB	N	AB
O_c	7	4	50	60	43	36	6.1	9.0
O_c_u	23	50	51	50	26	0	1.1	–

treated sample (Table 6). In sample O_c_u, the relative content of low-molecular-mass *n*-alkylbenzenes increases, but the amount of the medium-molecular-mass group decreases; high-molecular-mass *n*-alkylbenzenes are not detected. After the UST, the ratio of the high- to low-molecular-mass group decreases for both naphthenes and *n*-alkylbenzenes.

CONCLUSION

The action of physical fields on high-wax crude oil requires performing laboratory studies allowing prediction of changes in its properties such as viscosity and congealing point and of possible catastrophic consequences in the course of petroleum extraction and transportation in case of intense formation of paraffin plugs, which can cause failure of pumping stations and pipeline accidents. Ultrasonic treatment of the high-wax crude oil sample unambiguously leads to considerable changes in the structural and mechanical properties. The viscosity of the ultrasonically treated crude oil at low shear rates increases by a factor of more than 5 at 22°C, and the specific energy of the break of the disperse system is 1.7 times higher. The ultrasonic treatment of the crude oil leads to an almost twofold increase in the precipitate amount with the formation of shorter needle-like crystals. According to the GC-MS data, the content of naphthenes and *n*-alkylbenzenes in the ultrasonically treated crude oil decreases, which can lead to an increase in the congealing point. The positive effect of the ultrasonic treatment is a decrease in the relative content of high-molecular-mass *n*-alkanes in the precipitates. The GC-MS data for the oil fraction of the samples agree with the IR data.

AUTHOR INFORMATION

G.I. Volkova, ORCID: https://orcid.org/0000-0003-3986-8555

D.A. Zubarev, ORCID: https://orcid.org/0009-0002-3681-9264

P.B. Kadychagov, ORCID: https://orcid.org/0000-0002-8756-5164

FUNDING

The study was funded by the budget of the Institute of Petroleum Chemistry, Siberian Branch, Russian Academy of Sciences.

CONFLICT OF INTEREST

The authors declare no conflict of interest requiring disclosure in this article.

REFERENCES

1. Xie, Y., Zhang, J., Ma, C., Chen, C., Huang, Q., Li, Z., Ding, Y., Li, H., and Han, S., *Fuel,* 2020, vol. 267, Art. ID 117161. https://doi.org/10.1016/j.fuel.2020.117161
2. https://www.iea.org/oilmarketreport/omrpublic/
3. Chala, G.T., Sulaiman, S.A., and Japper-Jaafar, A., *J. Non-Newtonian Fluid Mech*., 2018, vol. 251, pp. 69–87. https://doi.org/10.1016/j.jnnfm.2017.11.008
4. Garris, N.A., Poletaeva, O.Yu., and Bakiev, T.A., *Transp. Khran. Nefteprod. Uglevodor. Syr'ya*, 2020, no. 3, pp. 64–67. https://doi.org/10.24411/0131-4270-2020-10311
5. https://neftegaz.ru/tech-library/geologiya-poleznykh-iskopaemykh/147767-trudnoizvlekaemye-zapasy-nefti-triz/
6. *State Report: State of the Art and Use of Mineral Resources in the Russian Federation in 2020*, Moscow: Ministry of Natural Resources and Ecology of the Russian Federation, Federal Agency of Subsoil Use, 2021.
7. Struchkov, I.A., Roschin, P.V., Litvin, V.T., Ol'khovskaya, V.A., and Kalinin, E.S., *J. Petrol. Explor. Prod. Technol.*, 2020, vol. 10, pp. 755–767. https://doi.org/10.1007/s13202-019-00779-2
8. Ansari, F., Shinde, S.B., Paso, K.G., Sjöblom, J., and Kumar, L., *Energy Fuels*, 2022, vol. 36, pp. 3372–3393. https://doi.org/10.1021/acs.energyfuels.1c03747
9. Litvinets, I.V., Yudina, N.V., Loskutova, Yu.V., and Prozorova, I.V., *Neft. Khoz*., 2018, no. 2, pp. 85–89. https://doi.org/10.24887/0028-2448-2018-2-85-89
10. Afra, S., Hisham, A., Nasr-El-Din, H., Socci, D., and Zheng, C., *Fuel*, 2018, vol. 220, pp. 481–489. https://doi.org/10.1016/j.fuel.2018.01.111
11. Kazantsev, O.A., Orekhov, D.V., Samodurova, S.I., Kamorin, D.M., Moikin, A.A., Volkova, G.I., Prozorova, I.V., Litvinets, I.V., and Medzhibovskii, A.S., *Petrol. Chem*., 2016, no. 1, pp. 68–72. https://doi.org/10.1134/S0965544115060079
12. Musina, N.S. and Maryutina, T.A., *J. Anal. Chem*., 2016, no. 1, pp. 27–34. https://doi.org/10.1134/S1061934816010081
13. Huang, Q., Li, H., Zhuang, Yu., Ding, Y., Ma, C., Chen, C., Xie, Y., Liang, H., Han, S., and Zhang, J., *Fuel*, 2021, vol. 283, Art. ID 1119345. https://doi.org/10.1016/j.fuel.2020.119345
14. Loskutova, Yu.V., Yudina, N.V., and Daneker, V.A., *Izv. Vyssh. Uchebn. Zaved., Ser. Khim. Khim. Tekhnol.*, 2019, no. 1, pp. 70–77. https://doi.org/10.6060/ivkkt.20196201.5766
15. Cui, J., Zhang, Z., Liu, X., Liu, L., and Peng, J., *Fuel*, 2020, vol. 263, ID 16638. https://doi.org/10.1016/j.fuel.2019.116638
16. Hofstatter, H., Pavlov, M.V., and Mastobaev, B.N., *SOCAR Proc*., 2014, no. 4, pp. 35–39. https://doi.org/10.5510/OGP20140400219
17. Barkalova, E.M., *Problems of Subsoil Geology and Development: Proc. XVII Int. Scientific Symp. of Young Scientists, Named after Academician M.A. Usov: "Problems of Subsoil Geology and Development," Dedicated to the 160th Birthday Anniversary of Academician V.A. Obruchev and 140th Anniversary of Academician M.A. Usov*, Tomsk: Tomsk Polytechnic Univ., 2020, pp. 545–547.
18. Volkova, G.I., Anufriev, R.V., and Yudina, N.V., *Neftekhimiya*, 2016, vol. 56, pp. 683–689. https://doi.org/10.1134/S0965544116080193
19. Volkova, G.I. and Morozova, A.V., *J. Phys. Conf. Ser.,* 2020, vol. 1611, no. 1, Art. ID 012018. https://doi.org/10.1088/1742-6596/1611/1/012018
20. Abramova, A., Abramov, V., Bayazitov, V., Gerasin, A., and Pashin, D., *Engeneering*, 2014, vol. 6, pp. 177–184.
21. Alhomadhi, E., Amro, M., and Almobarky, M., *J. King Saud Univ*., 2013, vol. 26, pp. 103–110. https://doi.org/10.1016/j.jksues.2013.04.002
22. Wang, Z., Fang, R., and Guo, H., *Ultrason. Sonochem*., 2020, vol. 60. https://doi.org/10.1016/j.ultsonch.2019.104791
23. Dengaev, A.V., Khelkhal, M.A., Getalov, A.A., Baimukhametov, G.F., Kayumov, A.A., Vakhin, A.V., and Gafurov, M.R., *Fluids*, 2023, vol. 8, no. 4, Art. ID 108. https://doi.org/10.3390/fluids8040108
24. *Sovremennye metody issledovaniya neftei (Spravochno-metodicheskoe posobie)* (Modern Methods for Studying Crude Oils (Methodical Handbook)), Bogomolov, A.I., Temyanko, M.B., and Khotyntseva, L.I., Eds., Leningrad: Nedra, 1984, p. 431.
25. Mullakaev, M.S., *Doctoral (Eng.) Dissertation*, Moscow: Moscow State Univ. of Environmental Engineering, 2011.
26. Morozova, A.V. and Volkova, G.I., *Chem. Sustain. Develop*., 2020, vol. 28, pp. 494–500. https://doi.org/10.15372/CSD20202570
27. Vinogradov, G.V. and Malkin, A.Ya., *Reologiya polimerov* (Polymer Rheology), Moscow: Khimiya, 1977.
28. Matveenko, V.N., Kirsanov, E.A., and Remizov, S.V., *Kolloidn. Zh*., 1994, vol. 56, no. 3, p. 393.